

Identification of molecular characteristics correlated with glioblastoma sensitivity to EGFR kinase inhibition through use of an intracranial xenograft test panel

Jann N. Sarkaria,¹ Lin Yang,¹ Patrick T. Grogan,¹ Gaspar J. Kitange,¹ Brett L. Carlson,¹ Mark A. Schroeder,¹ Evanthia Galanis,² Caterina Giannini,³ Wenting Wu,⁴ Eduard B. Dinca,⁵ and C. David James⁶

¹Department of Radiation Oncology, ²Division of Medical Oncology, ³Department of Laboratory Medicine and Pathology, ⁴Division of Biostatistics, and ⁵Neuroscience Graduate Program, Mayo Clinic, Rochester, Minnesota; and ⁶Department of Neurological Surgery and Brain Tumor Research Center, University of California, San Francisco, San Francisco, California

Abstract

In the current study, we examined a panel of serially passaged glioblastoma xenografts, in the context of an intracranial tumor therapy response model, to identify associations between glioblastoma molecular characteristics and tumor sensitivity to the epidermal growth factor receptor (EGFR) kinase inhibitor erlotinib. From an initial evaluation of 11 distinct glioblastoma xenografts, two erlotinib-sensitive tumors were identified, each having amplified EGFR and expressing wild-type PTEN. One of these tumors expressed truncated EGFRvIII, whereas the other expressed full-length EGFR. Subsequent cDNA sequence analysis revealed the latter tumor as expressing an EGFR sequence variant with arginine, rather than leucine, at amino acid position 62; this was the only EGFR sequence variant identified among the 11 xenografts, other than the aforementioned VIII sequence variant. EGFR cDNAs were then examined from 12 more xenografts to determine whether additional missense sequence alter-

ations were evident, and this analysis revealed one such case, expressing threonine, rather than alanine, at amino acid position 289 of the extracellular domain. This glioblastoma was also amplified for EGFR, but did not display significant erlotinib sensitivity, presumably due to its lacking PTEN expression. In total, our study identified two erlotinib-sensitive glioblastoma xenografts, with the common molecular characteristics shared by each being the expression of wild-type PTEN in combination with the expression of amplified and aberrant EGFR. [Mol Cancer Ther 2007;6(3):1167–74]

Introduction

Epidermal growth factor receptor (EGFR) inhibitors have experienced substantial application to the treatment of cancers for which increased EGFR signaling is thought to contribute to tumor-malignant behavior. However, only subgroups of tumors, for a specific type of cancer, have proven responsive to EGFR inhibitor therapy, and defining the molecular characteristics that predict individual tumor responsiveness has not been achieved in most instances. The notable exception, with respect to this point, is the observed EGFR kinase inhibitor responsiveness of lung cancers harboring EGFR kinase domain mutations (1).

Glioblastoma multiforme is the most common and malignant primary central nervous system cancer, and amplification-associated high-level expression of EGFR is observed in 30% to 40% of these tumors (2–4). The contribution of EGFR overexpression to the malignant behavior of glioblastoma has prompted several groups to test small molecule EGFR kinase inhibitors in patients with newly diagnosed as well as recurrent glioblastoma (5–7). Because of the biological parallels between EGFR amplification in glioblastoma and HER2 amplification in breast cancer, in combination with the observation that amplification-driven HER2 overexpression confers tumor sensitivity to anti-HER2 antibody therapy (8), there has been significant anticipation of high-level amplification-associated expression of EGFR denoting a subset of glioblastomas that are responsive to EGFR-directed therapies (9, 10).

Recently published laboratory-correlative components of clinical trials have generated mixed interpretations regarding the molecular characteristics associated with individual glioblastoma responsiveness to EGFR kinase inhibition. An initial report highlighted EGFR amplification and tumor phospho-Akt levels as key molecular markers for predicting response (5). A subsequent study indicated tumor positivity for EGFRvIII, a mutant and constitutively activated form of EGFR (11, 12) that is expressed in a

Received 11/9/06; revised 12/20/06; accepted 1/30/07.

Grant support: NIH NS49720 (C.D. James), CA097257 (C.D. James), CA108961 (J.N. Sarkaria, E. Galanis, and C. Giannini), CA25224 (J.N. Sarkaria, E. Galanis, and C. Giannini), and CA114740 (J.N. Sarkaria, E. Galanis, and C. Giannini); American Cancer Society Research Scholar Grant (J.N. Sarkaria); and Accelerate Brain Cancer Cure (J.N. Sarkaria and C.D. James).

The costs of publication of this article were defrayed in part by the payment of page charges. This article must therefore be hereby marked *advertisement* in accordance with 18 U.S.C. Section 1734 solely to indicate this fact.

Requests for reprints: C. David James, Department of Neurological Surgery, University of California, San Francisco, Room HSW 792, 513 Parnassus Avenue, San Francisco, CA 94143. Phone: 415-476-5876. E-mail: david.james@ucsf.edu

Copyright © 2007 American Association for Cancer Research.

doi:10.1158/1535-7163.MCT-06-0691

significant fraction of glioblastoma (13, 14), in combination with tumor retention of PTEN expression, as forming a molecular signature associated with tumor responsiveness to EGFR kinase inhibition (15). A third study, using immunoblot and EGFR kinase domain cDNA sequence analysis of patient surgical specimens, was unable to identify specific tumor molecular characteristics that predicted for responsiveness to EGFR kinase inhibitors (16). Finally, and most recently, the results of a multi-institutional study have shown that EGFR missense mutations, and consequent amino acid substitutions in the receptor extracellular domain, are potentially important towards conferring tumor sensitivity to EGFR small molecule inhibition (17).

In the current report, a distinct approach has been applied to the identification of molecular characteristics associated with glioblastoma sensitivity to EGFR kinase inhibitors. Here, we have used a panel of serially propagated glioblastoma xenografts, shown to maintain corresponding patient tumor morphologic and molecular characteristics including EGFR amplification (18), to evaluate the survival benefit of erlotinib that is administered orally in mice with established intracranial xenografts. Our correlative molecular analyses for these animal survival experiments support tumor expression of wild-type PTEN in combination with amplification of aberrant EGFR as being key characteristics of erlotinib-sensitive tumors.

Materials and Methods

Xenograft Information

Each of the 12 serially passaged xenografts used in this study were derived from tumors from different patients. Molecular genetic alterations and corresponding patient tumor histopathologic classifications for 10 of these xenografts have been previously described (19): 2 additional xenografts not previously reported, GS 22 and GBM 26, diagnosed as gliosarcoma and glioblastoma, respectively, have been included in the current investigation. All patients consented to the use of their tumor tissue in support of this research, and the use of the patient tissues received prior institutional review board authorization.

Orthotopic Xenograft Model and Therapy Response Experiments

All xenograft therapy evaluations were conducted using an orthotopic tumor model and a protocol approved by the Mayo Institutional Animal Care and Use Committee. In brief, flank tumor xenografts were harvested, mechanically disaggregated, and grown in short-term cell culture (5–14 days) in DMEM supplemented with 2.5% fetal bovine serum, 1% penicillin, and 1% streptomycin. Cells were harvested by trypsinization and injected into the right basal ganglia of anesthetized athymic nude mice (Ncr-*nu/nu*; National Cancer Institute, Frederick, MD). Mice were positioned for injection using a small animal stereotactic frame (ASI Instruments, Houston, TX), with each mouse receiving 10 μ L injections containing either 3×10^5 or 1×10^6 cells. Prior to treatment initiation, animals were

randomized to treatment and placebo/control groups of 5 to 10 mice each. EGFR kinase inhibitor therapy was initiated 2 weeks before the time mice were expected to become moribund, as established through preliminary studies with each xenograft line. Erlotinib (courtesy of Dr. Ken Iwata; OSI Pharmaceuticals, Melville, NY) was administered by oral gavage (either 100 or 150 mg/kg daily, with methyl cellulose used as the carrier) until mice became moribund, or until 4 weeks of treatment were completed (five times a week, maximum 20 administrations total). All mice used for therapy response evaluations were observed daily and euthanized at the time of reaching a moribund condition.

Immunoblotting

Flank tumor or microdissected intracranial tumor tissues were lysed in buffer A [50 mmol/L HEPES (pH 7.6), 30 mmol/L NaPPi, 10 mmol/L NaF, 150 mmol/L NaCl, 1 mmol/L EDTA, 1% Triton X-100, 10 ng/mL aprotinin, 10 ng/mL pepstatin, 10 ng/mL leupeptin, 20 mmol/L microcystin, 0.1 mmol/L phenylmethylsulfonyl fluoride, and 1 mmol/L sodium orthovanadate]. Lysates were cleared of insoluble material by centrifugation. Samples were boiled in SDS sample buffer, equal amounts of protein were loaded and electrophoresed through SDS-PAGE gels, and resolved proteins were transferred to Immobilon-P membranes (Millipore, Billerica, MA). Membranes were blocked with 5% milk dissolved in TBS containing 0.02% Tween 20, and then incubated with primary antibody diluted in the same buffer. After washing, membranes were incubated with either goat anti-rabbit (Cell Signaling, Danvers, MA) or goat anti-mouse (Pierce, Rockford, IL) antibodies conjugated to horseradish peroxidase. Blots were developed with Super Signal Chemiluminescence reagent (Pierce). Immunoblotting was done with phospho-specific antibodies first and then membranes were stripped and reprobed with the relevant antibodies against the corresponding total protein. Antibodies used in this study for the detection of total EGFR, phospho-EGFR, total PTEN, total Erk, phospho-T202/Y204 Erk, total Akt, and phospho-S473 Akt, were obtained from Cell Signaling; antibody for detection of β -actin was obtained from Sigma (St. Louis, MO).

Immunohistochemistry

Brains from mice with intracranial tumor were resected, and then bisected along the needle tract used for injecting the tumor cells. Half of each bisected brain was placed in formalin and subsequently embedded in paraffin. The other half of each brain was frozen in optimal cutting temperature medium. For the determination of MIB-1 labeling, formalin-fixed, paraffin-embedded tissues were sectioned, and mounted sections were deparaffinized prior to antigen retrieval in 1 mmol/L of EDTA (pH 8.0) at 100°C. Sections were incubated in ethanol with 3% H₂O₂ and then incubated with a 1:100 dilution of MIB-1 monoclonal antibody. After washing, sections were incubated with a secondary antibody conjugated with a polymer-based Hrp/DAB molecule (EnVision+, DAKO Cytomation, Carpinteria, CA), developed with 3,3'-diaminobenzidine, and then counterstained with modified

Schmidt's hematoxylin. MIB-1 staining was visualized by light microscopy. For determination of MIB-1 labeling index, digital images of five high-powered fields were obtained for each tumor, and the fraction of the area within those fields having MIB-1 staining was determined by image analysis using the KS400 image analysis software (Carl Zeiss, Inc., Oberkochen, Germany).

For CD31 analysis, frozen sections of corresponding optimal cutting temperature medium-embedded tissues were fixed in acetone and stained with rat anti-mouse CD31 antibody (clone MEC13.3; BD PharMingen, San Jose, CA) at a 1:50 dilution. Slides were subsequently processed as described for MIB-1 staining. The number of CD31-staining microvessels for each tumor section were quantified in three fields at 60 \times magnification.

Terminal nucleotidyl transferase-mediated nick end labeling (TUNEL) analysis was done using the ApopTag Plus Peroxidase In Situ Apoptosis detection kit (Millipore, Temecula, CA), according to the directions of the manufacturer. To determine the extent of TUNEL positivity, digital images of five high-powered fields were obtained for each tumor, and the fraction of the area with TUNEL staining was determined by image analysis using the KS400 image analysis software.

Tumor Cell Modification with Luciferase Reporter and Use in Bioluminescence Imaging

To enable noninvasive monitoring of intracranial tumor growth and response to erlotinib, short-term explant cultures of GBM 39 cells were transduced with HIV1-based lentiviral vectors expressing firefly luciferase (Fluc). Lentiviral vectors were generated by transfection of 293T cells with plasmids encoding the vesicular stomatitis virus G envelope, gag-pol, and Fluc (generously provided by Dr. Y. Ikeda, Mayo Clinic, Rochester, MN; ref. 20). Conditioned medium containing viral vectors were harvested 48 h post-transfection, filtered (0.45 μ m), and frozen until use. GBM 39 cells were transduced using viral supernatants, and expression of Fluc was confirmed by measuring cellular luciferase activity (IVIS 200; Xenogen Corporation, Alameda, CA). Fluc-modified GBM 39 cells were then collected and used to establish intracranial tumors that were monitored for erlotinib response by longitudinal bioluminescence imaging, as well as by survival analysis.

Molecular Genetic Analysis of Xenograft EGFR and PTEN Status

Approaches used for the determination of individual xenograft EGFR amplification as well as PTEN genetic status have been previously described (21–23). Sequence analysis of EGFR and PTEN was done for the entire coding region of each gene.

Statistical Analysis

The Kaplan-Meier estimator (24) was used to generate the survival curves and to estimate the median survival values. Differences between survival curves were compared using a log-rank test (25). Student's *t* test was used to evaluate differences between placebo and treatment groups with relation to MIB-1 labeling index, CD31-positive microvessel density, and TUNEL positivity.

Results

An orthotopic xenograft therapy response model was used to compare the erlotinib sensitivity of two xenograft lines, GBM 12 and GBM 14, with disparate EGFR amplification and PTEN status (Fig. 1). Survival benefit results for this comparison were consistent with interpretations associated with recently published glioblastoma clinical trials indicating that tumor EGFR and PTEN genetic status are important determinants of tumor response (5, 15). Specifically, erlotinib treatment was associated with a significant prolongation in survival for mice with established intracranial GBM 12 (Fig. 2A), which expresses wild-type PTEN and high levels of amplification-associated EGFR (Fig. 1). In contrast, mice with intracranial GBM 14, which lacks EGFR amplification and does not express PTEN protein due to homozygous PTEN gene inactivation (Fig. 1), experienced no survival benefit from erlotinib treatment (Fig. 2B).

The above results motivated a subsequent examination of nine more xenografts to further investigate the relationship between tumor EGFR + PTEN status and erlotinib sensitivity. From the results of these survival analyses (Table 1), one additional tumor was determined as displaying significant sensitivity to erlotinib: GBM 39, which expresses wild-type PTEN protein and high levels of amplification-associated EGFR (Fig. 1). Thus, the PTEN and EGFR amplification status of the two tumors showing erlotinib sensitivity are identical, although amplified EGFR in GBM 12 is full-length protein rather than the truncated EGFRvIII mutant in GBM 39. Tumor phospho-Akt and phospho-Erk content, which are molecular characteristics

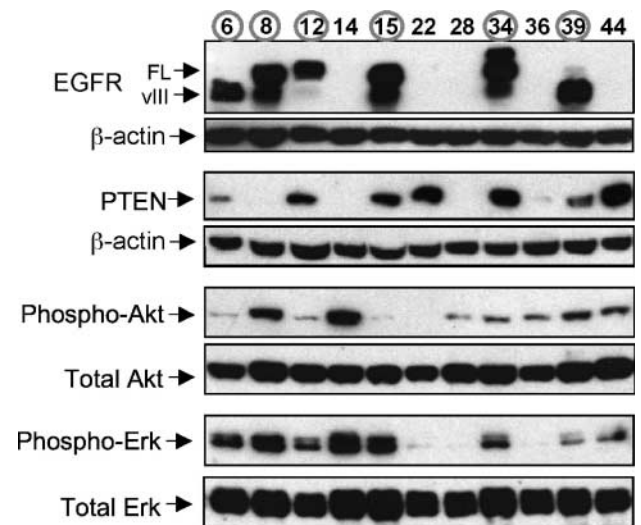


Figure 1. Xenograft immunoblot results of signaling mediators that potentially influence tumor erlotinib response. S.c. flank tumors, for the initial 11 xenografts examined for erlotinib response (Table 1), were harvested and used to prepare cleared lysates. Equal amounts of total protein from these lysates were electrophoresed and blot-transferred to polyvinylidene difluoride membranes. Membranes were probed with antibodies against the indicated proteins. Number of tumors with amplified and overexpressed EGFR are encircled (FL, full length; vIII, truncated variant III EGFR).

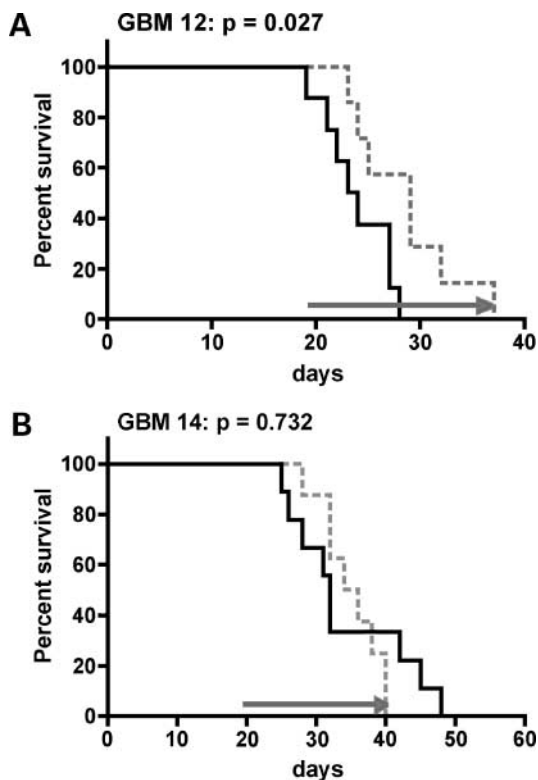


Figure 2. Contrasting erlotinib survival benefit in mice with distinct genetic subtypes of glioblastoma. Kaplan-Meier survival analysis was conducted for assessing erlotinib survival benefit, relative to placebo, for mice with established intracranial tumors from GBM 12 (A) or GBM 14 (B). Mice were randomly assigned to treatment groups and dosed by oral gavage (methylcellulose only or methylcellulose + erlotinib) until moribund. Arrows, the period of time over which treatments were administered (bottom). Significance levels for differences between control and treatment group survivals are indicated.

potentially important to glioblastoma sensitivity to erlotinib, did not show a clear association with tumor response to this EGFR kinase inhibitor (Fig. 1).

Survival results from GBM 15 and GBM 6, which have identical EGFR + PTEN status to that of GBM 12 and GBM 39, respectively (Fig. 1), did not indicate erlotinib sensitivity (Table 1). To investigate the basis of differential erlotinib response among these xenografts, mice with established intracranial tumors from either GBM 6, GBM 12, GBM 15, or GBM 39 were treated for 5 days with placebo or erlotinib, and then sections of whole brains from these mice were examined for immunohistochemical reactivity indicative of tumor cell proliferation (MIB-1). The results from this analysis revealed a substantial erlotinib antiproliferative effect for GBM 39 (78% reduction in MIB-1 labeling in erlotinib-treated mice; Fig. 3A and B), which is consistent with the significant erlotinib survival benefit experienced by mice with intracranial GBM 39 (Table 1). For the other three xenografts, however, the results suggested modest erlotinib antiproliferative effects that do not provide a clear explanation for erlotinib-associated survival benefit (GBM 12), or lack of survival benefit (GBM 6 and GBM 15). To

address the possibility that minor erlotinib-associated antiproliferative effects could be attributed to a lack of target inhibition, EGFR phosphorylation status was compared between microdissected intracranial GBM 15 from erlotinib-treated and untreated mice. The results of this analysis support erlotinib as inhibiting EGFR in intracranial GBM 15, as revealed by a lack of detectable phospho-EGFR in intracranial tumors from erlotinib-treated animals (Fig. 3C). Similar to the erlotinib proliferation effects for GBM 6, GBM 12, and GBM 15, erlotinib treatment was *not* associated with substantial differences in CD31-positive microvessel density (Fig. 3D), which would be indicative of an antiangiogenic effect, nor significant increases in TUNEL positivity (Fig. 3E), which would be indicative of apoptosis induction, in any of the four xenografts.

To address the reproducibility of the initial survival studies (Table 1), analyses of GBM 12 and GBM 39 were repeated, although using a higher daily dose of erlotinib in the case of GBM 12 (150 mg/kg, rather than the 100 mg/kg dose used in the initial experiment). For each tumor, mice treated with erlotinib again experienced significant survival benefit relative to corresponding control group mice ($P = 0.004$ for GBM 12; $P = 0.001$ for GBM 39). Other tumors examined a second time also yielded survival benefit results, the significance of which was consistent with those of the corresponding initial experiment, i.e., erlotinib treatment did not significantly extend the survival of mice with intracranial tumors established from xenografts GBM 14 or GBM 15 ($P = 0.71$ and 0.92 , respectively).

In the case of the second experiment with GBM 39, tumor cells were modified prior to intracranial injection by

Table 1. Xenograft erlotinib response results

| Tumor | EGFR | PTEN | Mean* | Δ Mean (%) [†] | P |
|-----------------------|--------------|------------------|---------------|--------------------------------|--------------|
| 6 | +vIII | Wild-type | 78/82 | 5 | 0.536 |
| 12[‡] | + | Wild-type | 24/29 | 21 | 0.027 |
| 15 | + | Wild-type | 43/45 | 5 | 0.683 |
| 34 | + | Wild-type | 103/115 | 12 | 0.860 |
| 39[‡] | +vIII | Wild-type | 88/121 | 38 | 0.014 |
| 8 | + | Null | 102/99 | -4 | 0.797 |
| 22 | - | Wild-type | 44/52 | 18 | 0.226 |
| 44 | - | Wild-type | 71/61 | -14 | 0.362 |
| 14 | - | Null | 34/35 | 3 | 0.732 |
| 28 | - | Null | 34/36 | 6 | 0.191 |
| 36 | - | Null | 123/112 | -9 | 0.445 |

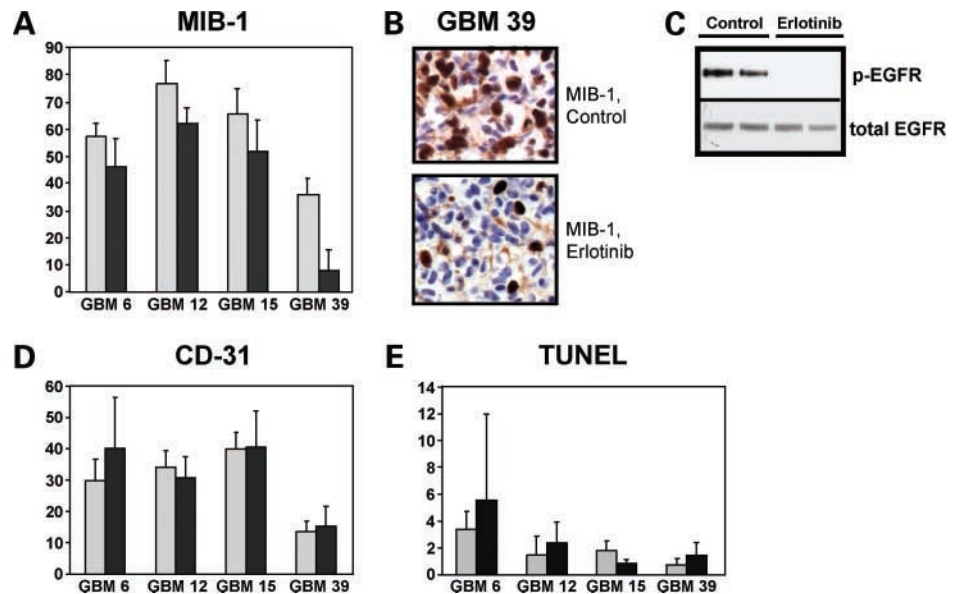
NOTE: Once a day administration (Monday to Friday), until symptomatic or for a maximum of 4 wks. Daily administration of 100 mg/kg for experiments with tumors 6, 8, 12, and 14; all others at 150 mg/kg daily.

*Mean values are in days; values to the left of each pair are for control groups, whereas values to the right are for erlotinib treatment groups. Equal numbers of control and treatment group mice were used in testing each xenograft, with not less than 5 nor more than 10 mice tested per group.

[†]Percentage of change in mean survival between control and erlotinib treatment groups.

[‡]Results in boldface are for tumors showing sensitivity to erlotinib, as indicated by the significant ($P < 0.05$) survival benefit for erlotinib-treated mice.

Figure 3. Effect of erlotinib therapy on proliferation, angiogenesis, apoptosis, and EGFR activation. Mice with established intracranial GBM 6, GBM 12, GBM 15, and GBM 39 tumors were assigned to placebo or erlotinib (150 mg/kg) treatment for 5 consecutive days prior to sacrifice. Intact brains were removed, sectioned, and processed for immunohistochemical analysis of markers associated with proliferation (**A** and **B**), angiogenesis (**D**), and apoptosis (**E**). **C**, pairs of mice with intracranial GBM 15 were either mock-treated or treated with five daily administrations of erlotinib prior to sacrifice and brain resection. Resected brains were mounted in optimal cutting temperature medium, and following the H&E staining of an initial frozen section to provide orientation, tumor cores were dissected for protein isolation and immunoblot analysis using antibodies against phospho- and total EGFR.



transduction with luciferase-encoding lentivirus (20), to allow bioluminescence monitoring of tumor response to erlotinib both during and following completion of treatment. The results of this monitoring show decreasing tumor luminescence after ~14 days of erlotinib therapy and increasing luminescence only after cessation of treatment (Fig. 4A and B). The decrease of luminescence in mice with intracranial GBM 39 was consistent with significant cyto-reduction resulting from sustained erlotinib administration. Because two of the nine GBM 39 treatment group mice became moribund while on therapy (see survival analysis; Fig. 4C), erlotinib treatment did not prevent all mice from succumbing to the effects of intracranial tumor burden. It is worth noting that the two mice that became moribund while on therapy had the highest pretreatment luminescence readings (data not shown), indicative of their having the most substantial tumor burden at initiation of therapy.

Because of the recent determination of EGFR extracellular domain missense mutations in a significant fraction of tumors from patients with glioblastoma, combined with the demonstration of these mutations conferring increased receptor sensitivity to inhibition by erlotinib (17), we sequenced EGFR cDNA from all xenografts examined in association with this investigation. In addition to the two cases having VIII extracellular domain sequence alterations (GBM 6 and GBM 39), GBM 12 cDNA revealed an alteration with consequent leucine-to-arginine change at amino acid 62; missense alterations in this region of EGFR cDNA have been previously noted (17). Unlike lung cancers, xenograft erlotinib sensitivity was not associated with kinase domain alterations, and in fact, there was no kinase domain alteration detected among any of the xenografts.

To further investigate potential relationships between extracellular domain missense alterations and glioblastoma

response to erlotinib, EGFR cDNAs from 12 additional glioblastoma xenograft lines were examined, and among these, one additional missense sequence variant was identified: GBM 26, which displays a missense alteration resulting in an alanine-to-threonine substitution at amino acid position 289 (Fig. 5A). Given this result, we evaluated the sensitivity of GBM 26 to erlotinib using the intracranial therapy response model, but found that erlotinib treatment did not significantly prolong the survival of mice with intracranial GBM 26 (Fig. 5B). Unlike GBM 12, however, GBM 26 lacks expression of PTEN (Fig. 5C) due to homozygous PTEN gene inactivation.

Discussion

The results of this investigation provide support for the importance of obtaining information on individual tumor molecular characteristics, and using such information as part of the decision-making process for treating patients with cancer. For the current study, our starting hypothesis was based on interpretations of recently published clinical trials involving patients with glioblastoma treated with the EGFR small molecule inhibitors erlotinib and gefitinib (5, 15). Collectively, the conclusions of these reports support EGFR amplification and/or mutation, and/or maintenance of wild-type PTEN function, and/or tumor phospho-Akt status as contributing to a molecular signature for glioblastomas that are most likely to benefit from EGFR small molecule inhibitor therapy.

In the current study, each of the two erlotinib-sensitive xenografts express high levels of EGFR variants due to corresponding amplification of aberrant EGFR genes, and these tumors additionally express wild-type PTEN. Inspection of phospho-Akt and phospho-Erk results for these tumors does not provide an obvious explanation for their erlotinib sensitivity, relative to other tumors with

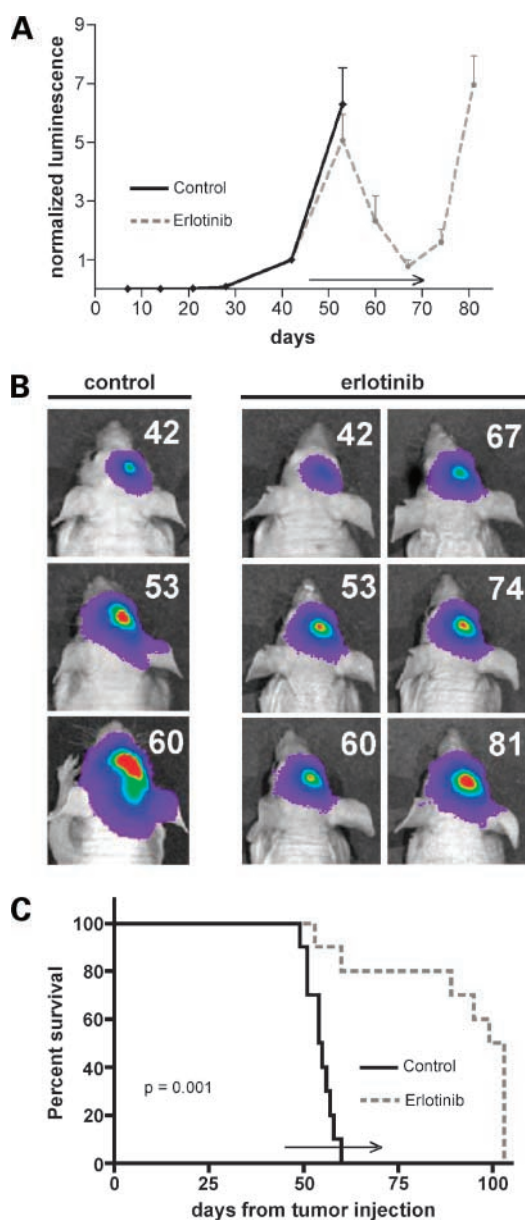


Figure 4. Bioluminescence monitoring and survival analysis of erlotinib-responsive tumor GBM 39. **A**, luminescence readings were converted to normalized values by dividing each mouse's luminescence readings with its corresponding maximal pretreatment luminescence reading recorded at day 42. Mean normalized bioluminescence and corresponding SE for control and treatment groups have been plotted for each imaging session and show decreasing normalized values for treatment group mice starting at day 60, which was 2 wks into the erlotinib administration regimen (arrow, treatment period). Treatment group luminescence is seen to increase following completion of the erlotinib administration regimen at day 71. Note that the mean normalized luminescence values for erlotinib treatment group mice are based on averages of 10 mice through day 53 imaging, and are based on averages of 8 mice from day 60 onward due to the deaths of 2 erlotinib treatment mice while on therapy. **B**, luminescence intensity overlays showing results for a single control group mouse and a single erlotinib treatment group mouse, with images recorded at days 42, 53, and 60 d for each, and additionally at days 67, 74, and 81 for the treatment group mouse. **C**, control versus treatment group survival comparison for this same experiment, showing substantial survival benefit for the group treated with erlotinib.

high-level amplification-associated expression of EGFR coupled with expression of wild-type PTEN, and that are not significantly sensitive to erlotinib (GBM 6 and GBM 15; Table 1; Fig. 1).

Our identification of an EGFR sequence variant in erlotinib-sensitive GBM 12 was motivated by the recent determination of EGFR extracellular domain missense alterations in surgical specimens from patients with glioblastoma, combined with the demonstration of these mutations being associated with enhanced erlotinib sensitivity in genetically modified cell lines (17). Following the identification of a GBM 12 sequence variant, we examined EGFR cDNA sequences from 12 more glioblastoma xenografts, and this analysis revealed one additional missense alteration in GBM 26, with an associated alanine-to-threonine amino acid change at position 289. Unlike GBM 12, mice with intracranial GBM 26 did not experience a significant survival benefit from erlotinib treatment (Fig. 5), thereby supporting the importance of tumor PTEN status, in addition to tumor EGFR amplification and mutation status, in determining glioblastoma response to erlotinib. The importance of EGFR amplification and extracellular domain alteration occurring in combination with tumor expression of wild-type PTEN was further reinforced by the erlotinib sensitivity of GBM 39, which expresses amplified EGFRvIII in combination with wild-type PTEN. However, because GBM 6, with identical EGFR and PTEN status as GBM 39, did not display erlotinib sensitivity, the combination of PTEN expression with EGFR amplification and mutation seems insufficient to confer obligate glioblastoma sensitivity to this small molecule inhibitor.

To address differences in biological response between erlotinib-sensitive and erlotinib-resistant glioblastomas, we examined intracranial tumors from erlotinib-treated mice for MIB-1, CD31, and TUNEL staining. The observed anti-proliferative, antiangiogenic, and proapoptotic responses were generally modest, except in the case of GBM 39 in which the MIB-1 results indicated substantial erlotinib antiproliferative effect (Fig. 3A and B). The use of bioluminescence imaging for the serial analysis of intracranial GBM 39 response to sustained erlotinib treatment revealed decreasing tumor luminescence during the course of treatment, with treatment group mean normalized luminescence values decreasing to <20% of the maximal treatment group mean normalized luminescence recorded at day 53 (Fig. 4A). This result may in fact indicate a proapoptotic, or otherwise, cytotoxic effect of sustained erlotinib treatment in GBM 39 that was not evident through immunohistochemical analysis following 5 days of treatment (Fig. 3E). The bioluminescence imaging result additionally suggests that sustained erlotinib treatment may have been needed to provide a rationale for the sensitivity of GBM 12, relative to GBM 6 and GBM 15, and that was not provided in association with a 5-day erlotinib treatment regimen (Fig. 3A, D, and E). In contrast, it is unlikely that an insufficient length of treatment contributed to a misinterpretation of xenograft erlotinib responsiveness because

each control versus treatment group survival comparison involved the use of a regimen that was sustained for 4 weeks, or until all treatment group mice had succumbed to tumor burden.

Our results suggest that EGFR amplification and mutation combined with tumor expression of functional PTEN are necessary but not sufficient for conferring glioblastoma sensitivity to EGFR kinase inhibition. Consequently, one could infer the existence of additional determinants of glioblastoma sensitivity to EGFR kinase inhibition yet to be identified. For instance, activating mutations of PIK3CA,

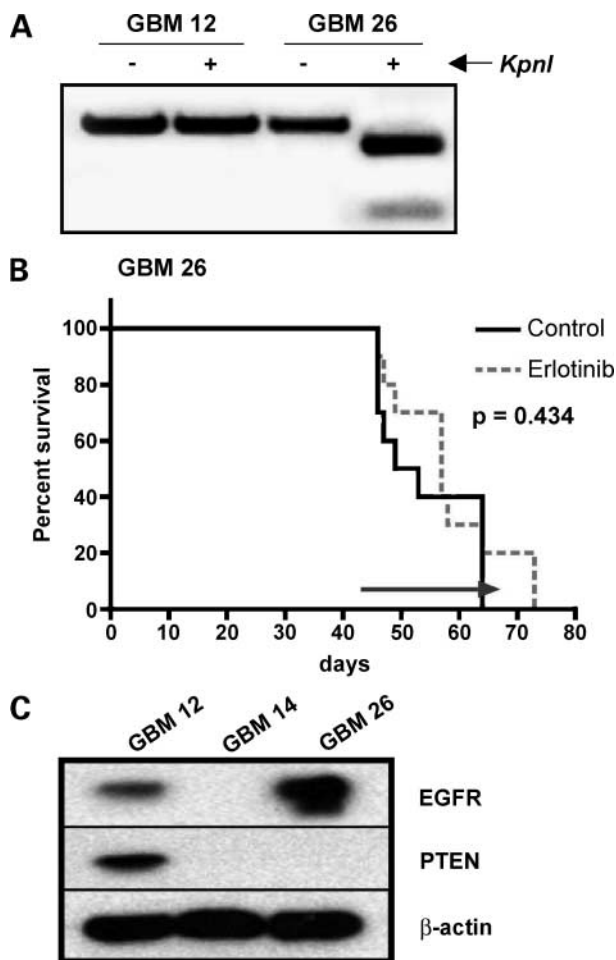


Figure 5. EGFR cDNA sequence variant in GBM 26, and erlotinib survival response analysis of mice with intracranial GBM 26 tumor. **A**, partial EGFR cDNAs from tumors GBM 12 and GBM 26 were amplified by reverse transcription-PCR, and amplification products were electrophoresed through a 1.0% agarose gel following treatment with (+) or without (-) *KpnI* restriction enzyme; a negative image of the corresponding ethidium bromide-stained gel is shown. The *KpnI*-treated sample from GBM 26 shows two fragments due to a G → A coding sequence variation at position 865 that creates a *KpnI* site. The complete loss of the full-length cDNA fragment in *KpnI*-treated GBM 26 indicates that the mRNA expressed in GBM 26 is entirely of a variant sequence. **B**, erlotinib survival response analysis of mice with intracranial GBM 26. Comparison of the survival curves supports a lack of survival benefit for erlotinib-treated mice ($P = 0.434$). **C**, immunoblot analysis showing EGFR amplification and lack of PTEN expression in GBM 26.

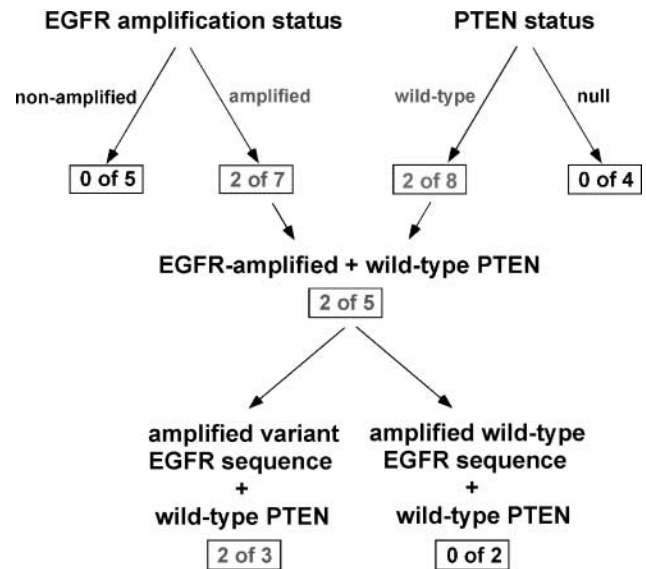


Figure 6. Diagram summarizing the genetic features of glioblastoma that should be useful for clinical decision-making regarding the inclusion or exclusion of patients with glioblastoma from treatment with EGFR kinase inhibitors. *Boxed numbers*, the proportion of xenografts in each genetic subgroup that displayed sensitivity to erlotinib (*gray*, responsive genetic subsets).

as recently shown in adult and pediatric glioblastomas (26), could account for tumor insensitivity to EGFR inhibition. Certainly, an expanded genomic analysis of these xenografts would be of benefit for increasing our understanding of the molecular basis of glioblastoma erlotinib response, and more generally, for providing insight regarding the basis of differential tumor response to any therapeutic. Nonetheless, the selection of patients with glioblastoma for erlotinib therapy based on the currently indicated molecular criteria (Fig. 6), should capture the majority of glioblastoma patients that would respond to EGFR kinase inhibitor therapy, and should greatly increase the positive response rate of patients receiving this therapy.

Beyond this conclusion, our study highlights the potential of using xenografts developed directly from patient surgical specimens for identifying molecular markers predictive of tumor response to therapy. Moreover, because the xenografts can be genetically modified *ex vivo*, such as was the case with GBM 39 cells used for bioluminescence imaging (Fig. 4), the significance of specific gene alterations to therapeutic response can be examined by restoring or suppressing gene function, and analyzing the therapeutic response consequences of such modifications.

References

- Pao W, Miller V, Zakowski M, et al. EGF receptor gene mutations are common in lung cancers from "never smokers" and are associated with sensitivity of tumors to gefitinib and erlotinib. *Proc Natl Acad Sci U S A* 2004;101:13306–11.
- Libermann TA, Nusbaum HR, Razon N, et al. Amplification, enhanced expression and possible rearrangement of EGF receptor gene in primary human brain tumours of glial origin. *Nature* 1985;313:144–7.

3. Wong AJ, Bigner SH, Bigner DD, Kinzler KW, Hamilton SR, Vogelstein B. Increased expression of the epidermal growth factor receptor gene in malignant gliomas is invariably associated with gene amplification. *Proc Natl Acad Sci U S A* 1987;84:6899–903.
4. Ekstrand AJ, James CD, Cavenee WK, Seliger B, Pettersson RF, Collins VP. Genes for epidermal growth factor receptor, transforming growth factor α , and epidermal growth factor and their expression in human gliomas *in vivo*. *Cancer Res* 1991;51:2164–72.
5. Haas-Kogan DA, Prados MD, Tihan T, et al. Epidermal growth factor receptor, protein kinase B/Akt, and glioma response to erlotinib. *J Natl Cancer Inst* 2005;97:880–7.
6. Reardon DA, Quinn JA, Vredenburgh JJ, et al. Phase 1 trial of gefitinib plus sirolimus in adults with recurrent malignant glioma. *Clin Cancer Res* 2006;12:860–8.
7. Krishnan S, Brown PD, Ballman KV, et al. Phase I trial of erlotinib with radiation therapy in patients with glioblastoma multiforme: results of North Central Cancer Treatment Group protocol N0177. *Int J Radiat Oncol Biol Phys* 2006;65:1192–9.
8. Pegram MD, Pauletti G, Slamon DJ. HER-2/neu as a predictive marker of response to breast cancer therapy. *Breast Cancer Res Treat* 1998;52:65–77.
9. Raizer JJ. HER1/EGFR tyrosine kinase inhibitors for the treatment of glioblastoma multiforme. *J Neurooncol* 2005;74:77–86.
10. Halatsch ME, Schmidt U, Behnke-Mursch J, Unterberg A, Wirtz CR. Epidermal growth factor receptor inhibition for the treatment of glioblastoma multiforme and other malignant brain tumours. *Cancer Treat Rev* 2006;32:74–89.
11. Nishikawa R, Ji XD, Harmon RC, et al. A mutant epidermal growth factor receptor common in human glioma confers enhanced tumorigenicity. *Proc Natl Acad Sci U S A* 1994;91:7727–31.
12. Ekstrand AJ, Longo N, Hamid ML, et al. Functional characterization of an EGF receptor with a truncated extracellular domain expressed in glioblastomas with EGFR gene amplification. *Oncogene* 1994;9:2313–20.
13. Aldape KD, Ballman K, Furth A, et al. Immunohistochemical detection of EGFRvIII in high malignancy grade astrocytomas and evaluation of prognostic significance. *J Neuropathol Exp Neurol* 2004;63:700–7.
14. Nishikawa R, Sugiyama T, Narita Y, Furnari F, Cavenee WK, Matsutani M. Immunohistochemical analysis of the mutant epidermal growth factor, δ EGFR, in glioblastoma. *Brain Tumor Pathol* 2004;21:53–6.
15. Mellingshoff IK, Wang MY, Vivanco I, et al. Molecular determinants of the response of glioblastomas to EGFR kinase inhibitors. *N Engl J Med* 2005;353:2012–24.
16. Lassman AB, Rossi MR, Raizer JJ, et al. Molecular study of malignant gliomas treated with epidermal growth factor receptor inhibitors: tissue analysis from North American Brain Tumor Consortium Trials 01-03 and 00-01. *Clin Cancer Res* 2005;11:7841–50.
17. Lee JC, Vivanco I, Beroukhi R, et al. Epidermal growth factor receptor activation in glioblastoma through novel missense mutations in the extracellular domain. *PLoS Med* 2006;3:e345.
18. Giannini C, Sarkaria JN, Saito A, et al. Patient tumor *EGFR* and *PDGFRA* gene amplifications retained in an invasive intracranial xenograft model of GBM. *Neuro-Oncol* 2005;7:164–76.
19. Sarkaria JN, Carlson BL, Schroeder MA, et al. Use of an Orthotopic Xenograft Model for Assessing the Effect of EGFR Amplification on Glioblastoma Radiation Response. *Clin Cancer Res* 2006;12:2264–71.
20. Hasegawa K, Pham L, O'Connor MK, Federspiel MJ, Russell SJ, Peng KW. Dual therapy of ovarian cancer using measles viruses expressing carcinoembryonic antigen and sodium iodide symporter. *Clin Cancer Res* 2006;12:1868–75.
21. James CD, Galanis E, Frederick L, et al. Tumor suppressor gene alterations in malignant gliomas: histopathological associations and prognostic evaluation. *Int J Oncol* 1999;15:547–53.
22. Pandita A, Aldape KD, Zadeh G, Guha A, James CD. Contrasting *in vivo* and *in vitro* fates of glioblastoma cell subpopulations with amplified EGFR. *Genes Chromosomes Cancer* 2004;39:29–36.
23. Frederick L, Wang XY, Eley G, James CD. Diversity and frequency of epidermal growth factor receptor mutations in human glioblastomas. *Cancer Res* 2000;60:1383–7.
24. Kaplan EL, Meier P. Non-parametric estimation from incomplete observations. *J Am Stat Assoc* 1958;53:457–81.
25. Peto R, Peto J. Asymptotically efficient rank invariant procedures. *J R Stat Soc Ser A Stat Soc* 1972;135:185–207.
26. Gallia GL, Rand V, Siu IM, et al. PIK3CA gene mutations in pediatric and adult glioblastoma multiforme. *Mol Cancer Res* 2006;4:709–14.

Molecular Cancer Therapeutics

Identification of molecular characteristics correlated with glioblastoma sensitivity to EGFR kinase inhibition through use of an intracranial xenograft test panel

Jann N. Sarkaria, Lin Yang, Patrick T. Grogan, et al.

Mol Cancer Ther 2007;6:1167-1174.

Updated version Access the most recent version of this article at:
<http://mct.aacrjournals.org/content/6/3/1167>

Cited articles This article cites 26 articles, 10 of which you can access for free at:
<http://mct.aacrjournals.org/content/6/3/1167.full#ref-list-1>

Citing articles This article has been cited by 54 HighWire-hosted articles. Access the articles at:
<http://mct.aacrjournals.org/content/6/3/1167.full#related-urls>

E-mail alerts [Sign up to receive free email-alerts](#) related to this article or journal.

Reprints and Subscriptions To order reprints of this article or to subscribe to the journal, contact the AACR Publications Department at pubs@aacr.org.

Permissions To request permission to re-use all or part of this article, use this link
<http://mct.aacrjournals.org/content/6/3/1167>.
Click on "Request Permissions" which will take you to the Copyright Clearance Center's (CCC) Rightslink site.